

Supporting Information of

**Heterogenization for polyoxometalates as solid catalysts in aerobic oxidation of glycerol**

Meilin Tao<sup>a,b</sup>, Yue Li<sup>a</sup>, Yiming Li<sup>a</sup>, Xueyan Zhang<sup>a</sup>, Yurii V Geletii<sup>b</sup>, Xiaohong Wang<sup>a,\*</sup>, Craig L Hill<sup>b,\*</sup>

<sup>a</sup> Key Lab of Polyoxometalate Science of Ministry of Education, Northeast Normal University, Changchun 130024, P. R. China, E-mail: wangxh665@nenu.edu.cn, Fax: 0086-431-85099759

<sup>b</sup> Department of Chemistry, Emory University, Atlanta, Georgia 30322, United States

**Experimental**

**Materials and reagents:** All the chemicals were of AR grade, which were obtained commercially and used without further purification.

**Instruments:** Elemental analysis was carried out using a Leeman Plasma Spec (I) ICP-ES. IR spectroscopy (4000-500 cm<sup>-1</sup>) was recorded in KBr discs on a Nicolet Magna 560 IR spectrometer. X-ray diffraction (XRD) patterns of the sample were collected on a Japan Rigaku Dmax 2000 X-ray diffractometer with Cu K $\alpha$  radiation ( $\lambda = 0.154178$  nm). The measurements were obtained in the step of 0.04° with account time of 0.5 s and in the 2θ rang of 5-90 °. SEM micrographs were recorded on a scan electron microscope (XL30 ESEM FEG 25kV). EDX spectra were obtained using 20 kV primary electron voltages to determine the composition of the samples. The redox potentials were measured by cyclic voltammetry (CV) on a CS Corrtest electrochemical workstation equipped with graphite powder (SP) and liquid paraffin (4:1) as electrodes and saturated calomel as reference electrode. Electrochemical measurements were performed in 0.1 M sulfuric acid solution. The <sup>31</sup>P MAS NMR spectra were obtained using a Bruker AM500 spectrometer at 202.5 MHz. The Lewis acidity was measured by IR spectra of adsorbed pyridine (Py-IR). The samples were exposed to the pyridine vapor for 12 h under vacuum (10<sup>-3</sup> Pa) at 60 °C before testing. The quantification of acidity was calculated by Lambert-Beer equation:

$$A = \frac{\epsilon \cdot w \cdot c}{s}$$

Where A is the absorbance (area in cm<sup>-1</sup>), ε is the extinction coefficient (m<sup>2</sup>/mol), w is the sample weight (kg), c is the concentration of acid (mol/kg or mmol/g), and s is the sample disk area (m<sup>2</sup>), respectively. The amount of L acid sites was estimated from the integrated area of the

adsorption bands at 1456 cm<sup>-1</sup>, respectively, using the extinction coefficient values based on the previous report [1].

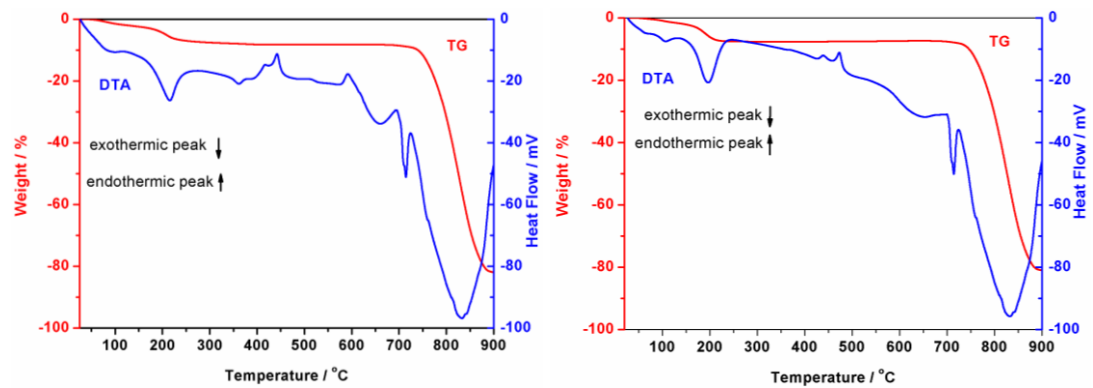


**Fig. S1.** TG and DTA of AlPMo<sub>12</sub> (left) HPMo<sub>11</sub>Al (right).

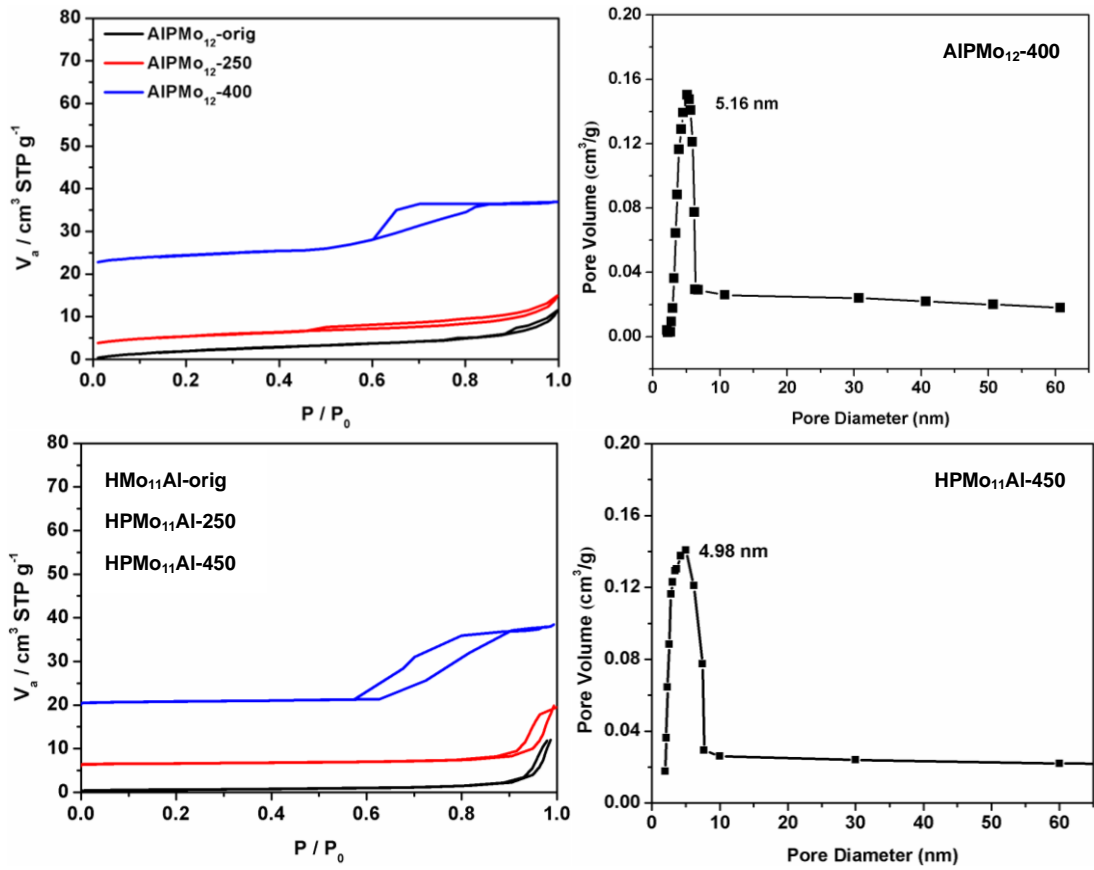


**Fig. S2.** N<sub>2</sub> sorption isotherms and the pore size distribution of AlPMo<sub>12</sub>-orig, AlPMo<sub>12</sub>-250, AlPMo<sub>12</sub>-400, HPMo<sub>11</sub>Al-orig, HPMo<sub>11</sub>Al-250, HPMo<sub>11</sub>Al-450.

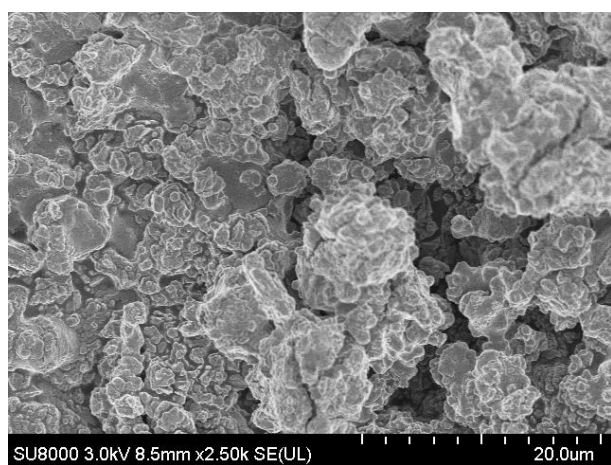


**Fig. S3.** SEM image of AlPMo<sub>12</sub>-400.

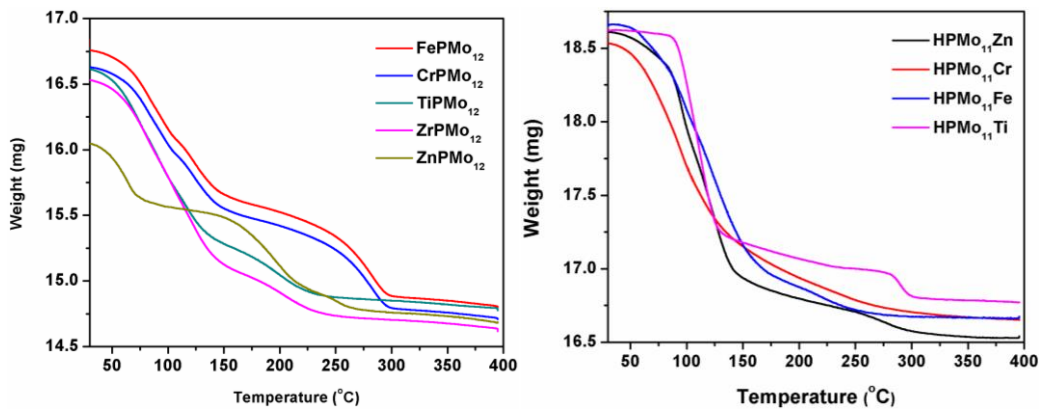


**Fig. S4.** TGA of LPMo<sub>12</sub> and HPMo<sub>11</sub>L catalysts. The POMs lose their crystallization water at around 250 °C. The data are consistent with the presence of 13 molecules of H<sub>2</sub>O per LPMo<sub>12</sub>, and 10 per HPMo<sub>11</sub>L before 300 °C.

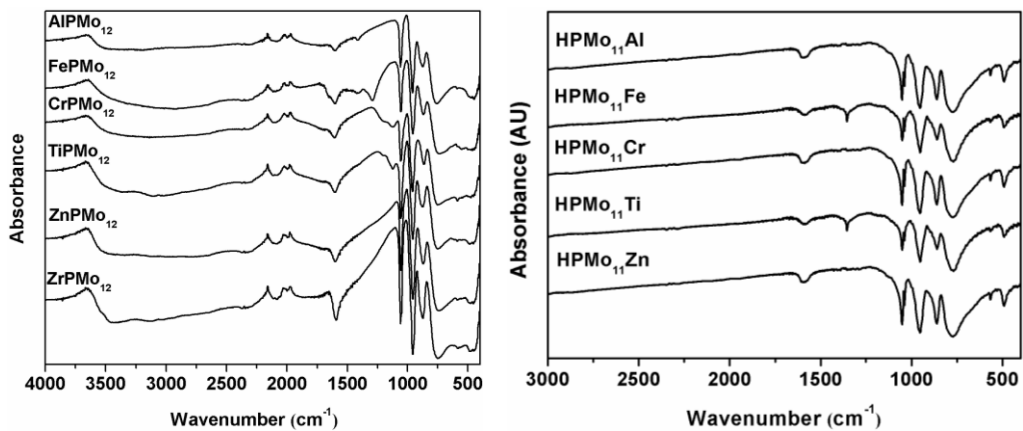


**Fig. S5.** FTIR spectra of homogeneous LPMo<sub>12</sub> and HPMo<sub>11</sub>L.

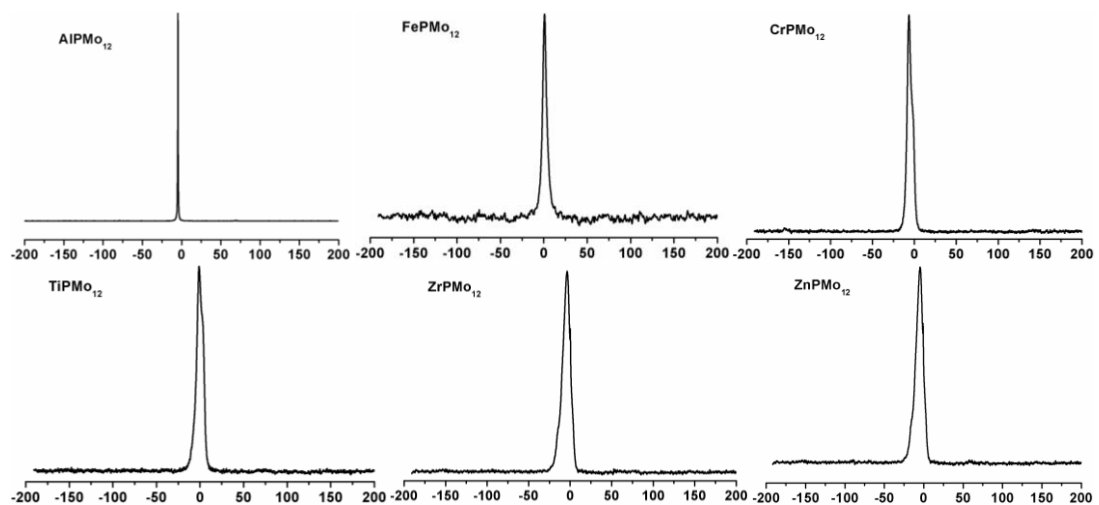


**Fig. S6.**  $^{31}\text{P}$  MAS NMR spectra of homogeneous LPMo<sub>12</sub>.

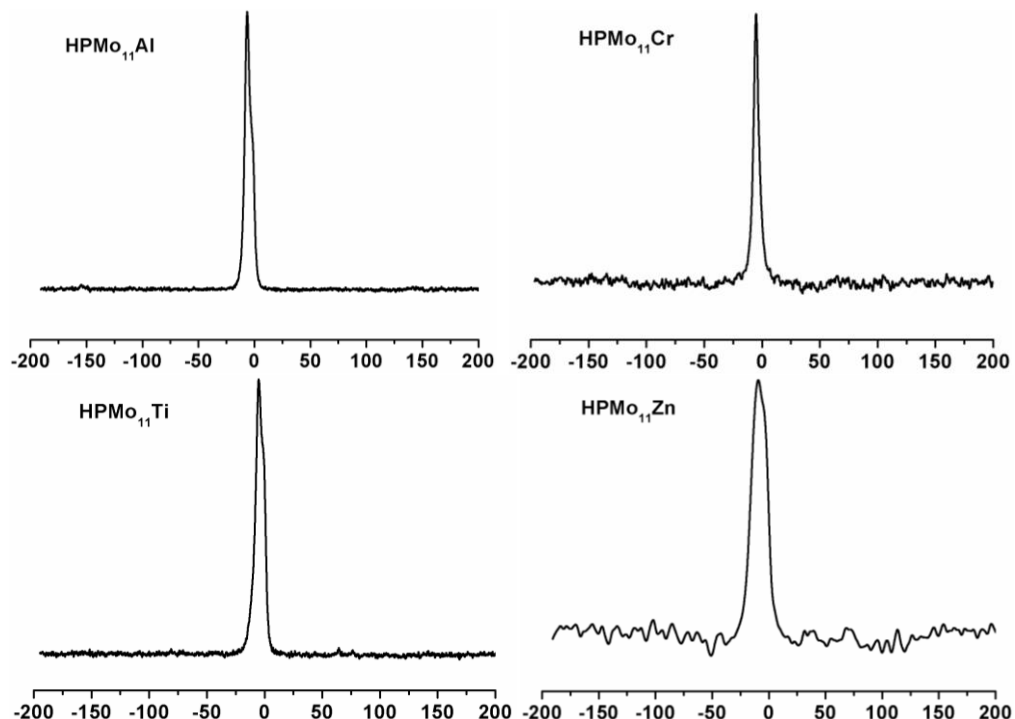


**Fig. S7.**  $^{31}\text{P}$  MAS NMR spectra of homogeneous HPMo<sub>11</sub>L.

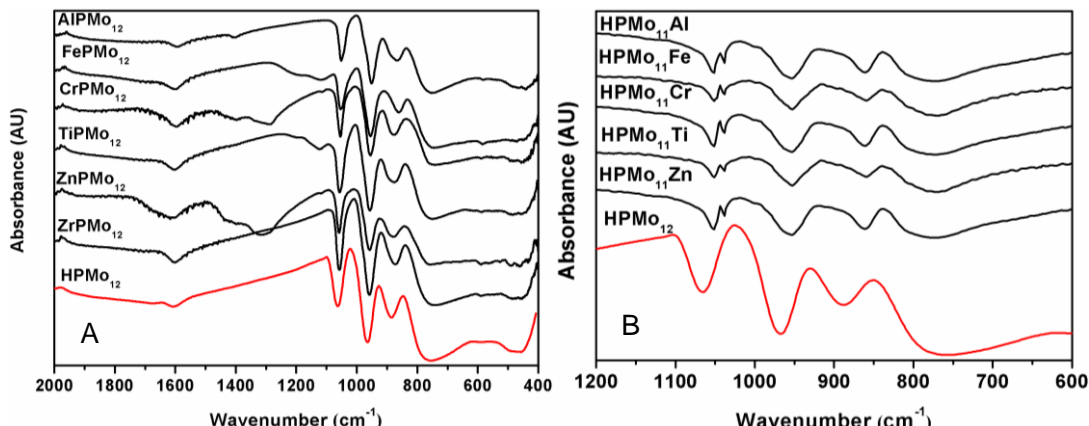


**Fig. S8.** (A) FTIR spectra of heterogeneous LPMo<sub>12</sub> catalysts, which exhibited four characteristic peaks at about 1057 cm<sup>-1</sup> (vas P-O), 958 cm<sup>-1</sup> (vas Mo=O), 873 cm<sup>-1</sup> (vas Mo-O-Mo), and 740 cm<sup>-1</sup> (vas Mo-O-Mo), red shifted with respect to parent H<sub>3</sub>PMo<sub>12</sub>O<sub>40</sub> (1060, 965, 882 and 748 cm<sup>-1</sup>).

(B) FTIR spectra of heterogeneous HPMo<sub>11</sub>L, which showed bands at 1051, 1038 (shoulder) (v (P-O)), 953 (v (Mo=O), terminal), 860 (v (Mo-O-L), corner-sharing octahedra), and 774 cm<sup>-1</sup> (v (Mo-O-L), edge-sharing octahedra) characteristic of the  $\alpha$ -Keggin structure similar to their parent H<sub>3</sub>PMo<sub>12</sub>O<sub>40</sub>. The splitting of v (P-O) band resulted from the decrease in the symmetry of PO<sub>4</sub> tetrahedron being caused by the L substitution for Mo in the PMo<sub>12</sub>O<sub>40</sub><sup>3-</sup> framework [2].

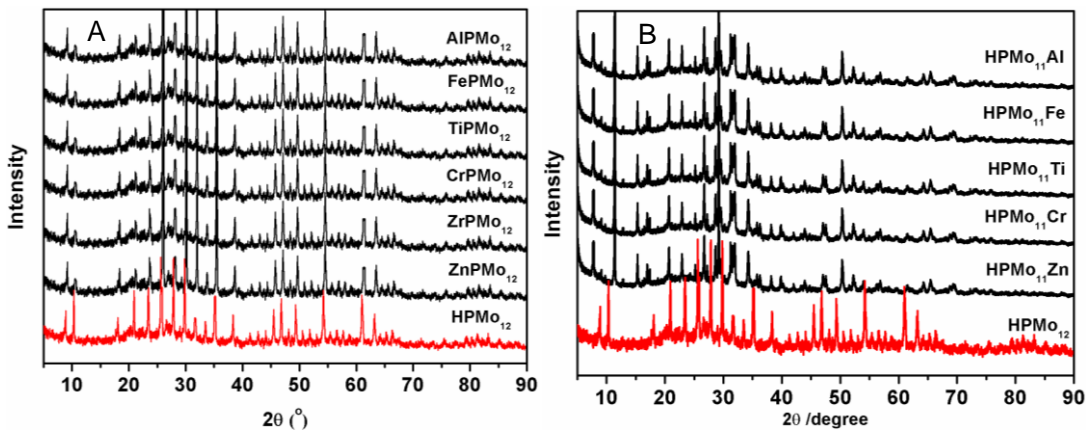


**Fig. S9.** XRD patterns of LPMo<sub>12</sub> (A) and HPMo<sub>11</sub>L (B). Compared with H<sub>3</sub>PMo<sub>12</sub>O<sub>40</sub> (10.35, 14.60, 17.85, 20.68, 23.11, 25.44, 31.22, and 34.67 °), some shifts appeared because of the replacement of proton in LPMo<sub>12</sub> and Mo in HPMo<sub>11</sub>L by metal ions, which confirmed the successful synthesis of LPMo<sub>12</sub> and HPMo<sub>11</sub>L.

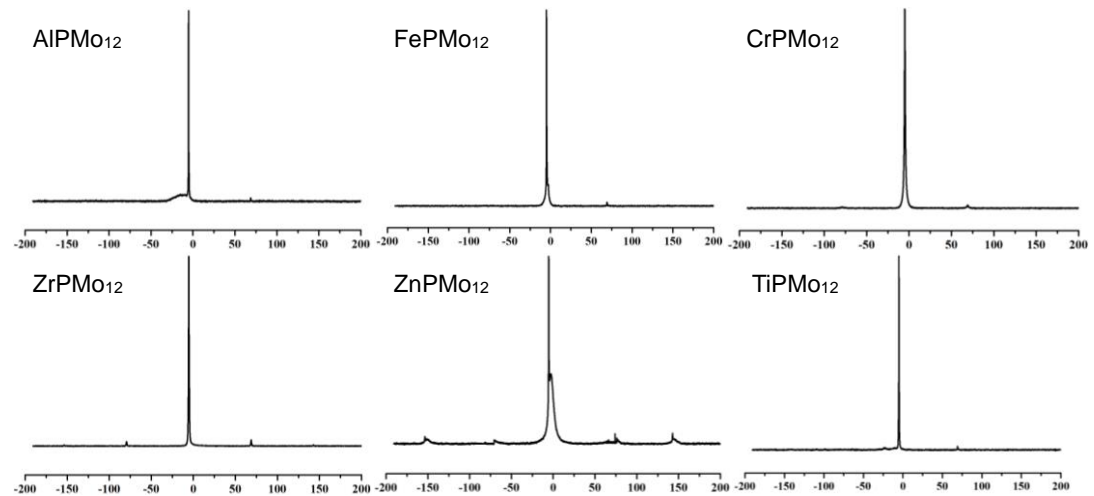


**Fig. S10.**  $^{31}\text{P}$  MAS NMR spectra of heterogeneous LPMo<sub>12</sub> catalysts. Their peaks at about -5.22 ppm with some shifts compared to H<sub>3</sub>PMo<sub>12</sub>O<sub>40</sub> at -5.43 ppm.

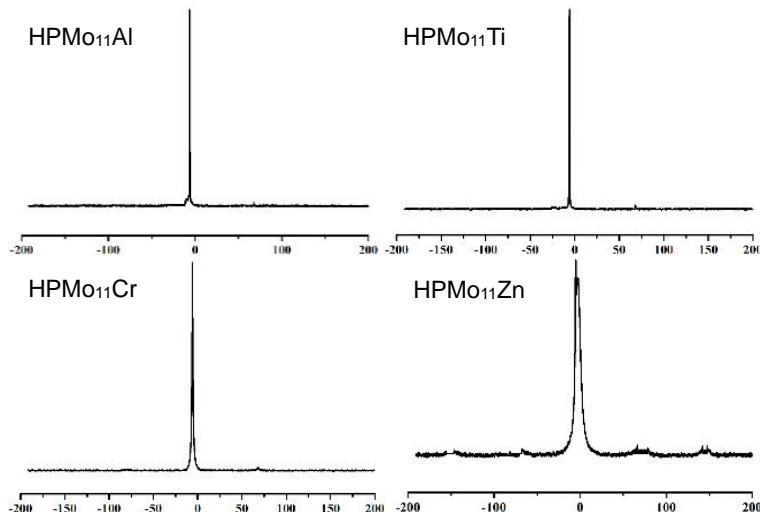
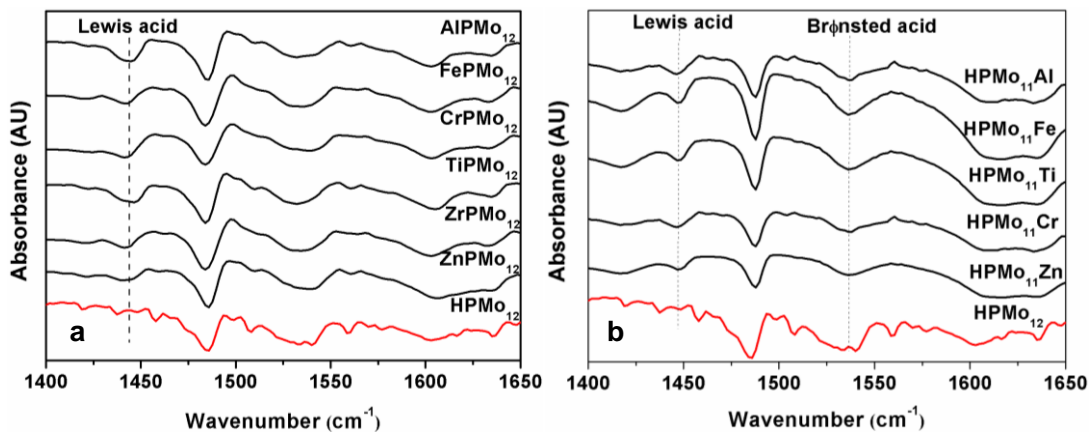
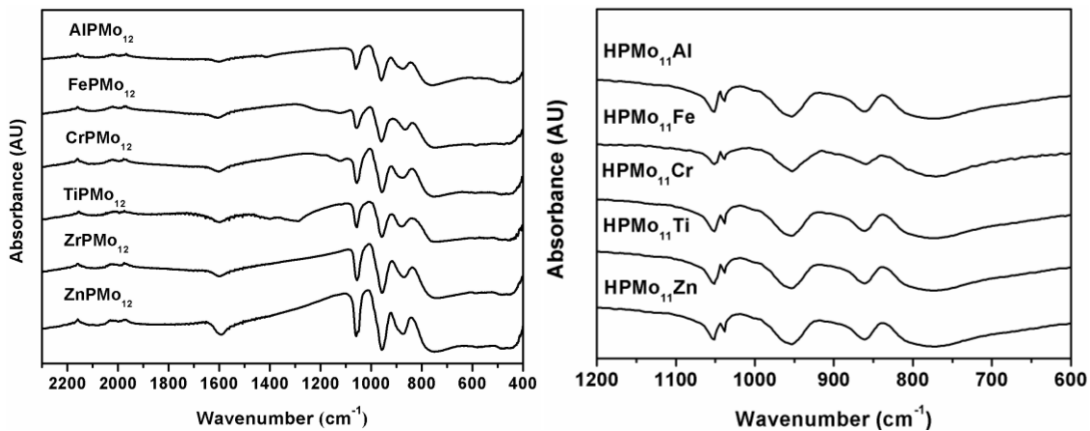


Fig. S11.  $^{31}\text{P}$  MAS NMR spectra of heterogeneous HPMo<sub>11</sub>L catalysts. They all presented one major peak around -5.80 ppm, which was assigned to PMo<sub>11</sub>L<sup>n-</sup> [3,4], some shifts occurred as the monosubstituted metal changed, which indicated that metal atoms were successfully inserted into vacancy of [PMo<sub>11</sub>O<sub>39</sub>]<sup>7-</sup> to form saturated POMs. No signals were observed for HPMoFe because of the presence of P-O-Fe<sup>3+</sup> (paramagnetic species) bond in the polyoxometalate structure in agreement with the literature [5].



**Fig. S12.** FTIR spectra of pyridine adsorption of  $\text{LPMo}_{12}$  (a) and  $\text{HPMo}_{11}\text{L}$  catalysts (b).

The Lewis acidity defined by molar number of pyridine absorbed by  $\text{LPMo}_{12}$ , which was measured by FT-IR spectroscopy. All the samples of  $\text{LPMo}_{12}$  have typical bands corresponding to strong Lewis acid bound pyridine, at around 1450 and 1610  $\text{cm}^{-1}$  [2]. The concentrations of Lewis acid sites were calculated from the bands at 1456  $\text{cm}^{-1}$  based on Lambert-Beer equation [1].



**Fig. S13.** FTIR spectra of LPMo<sub>12</sub> and HPMo<sub>11</sub>L catalysts after reaction.

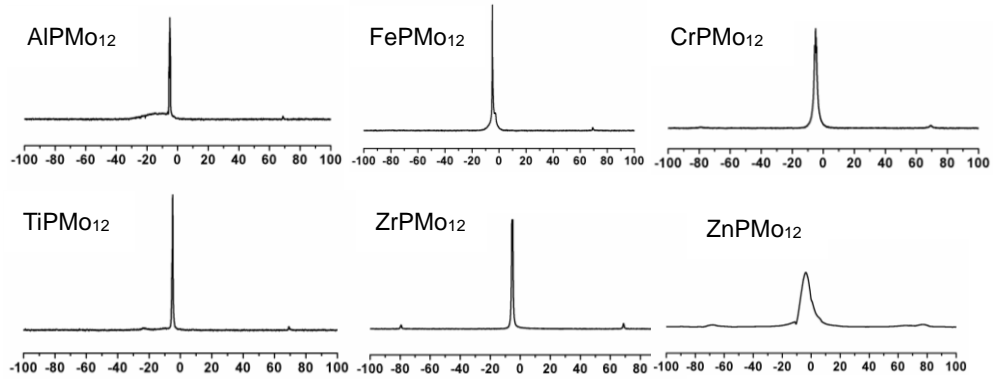


**Fig. S14.**  $^{31}\text{P}$  MAS NMR of LPMo<sub>12</sub> catalysts after reaction.

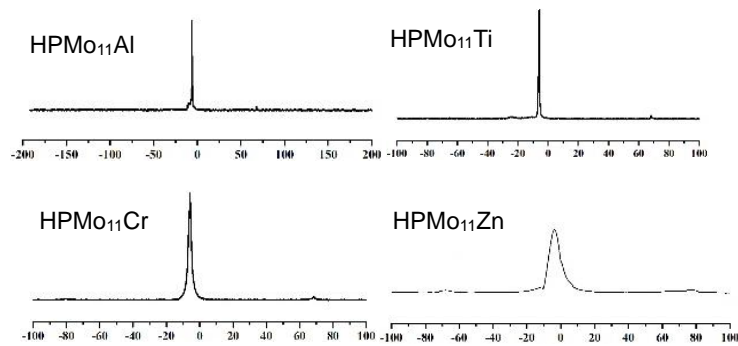


**Fig. S15.**  $^{31}\text{P}$  NMR of HPMo<sub>11</sub>L catalysts after reaction.

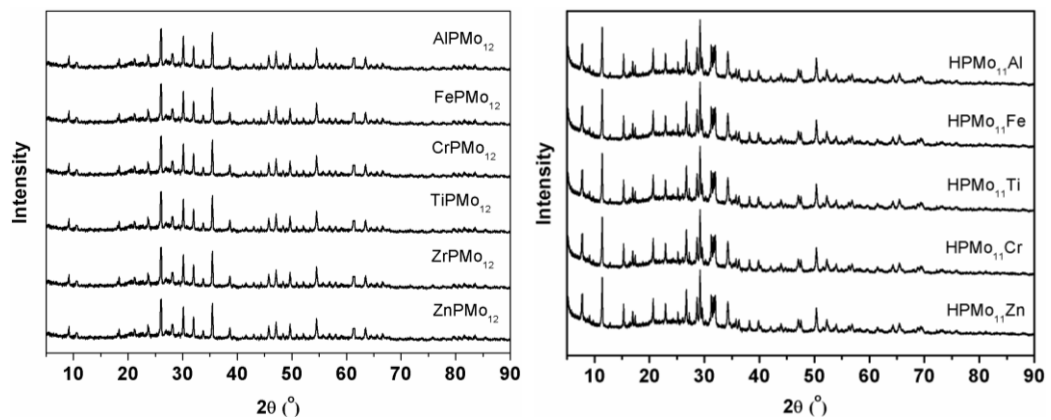


**Fig. S16.** XRD of LPMo<sub>12</sub> and HPMo<sub>11</sub>L catalysts after reaction

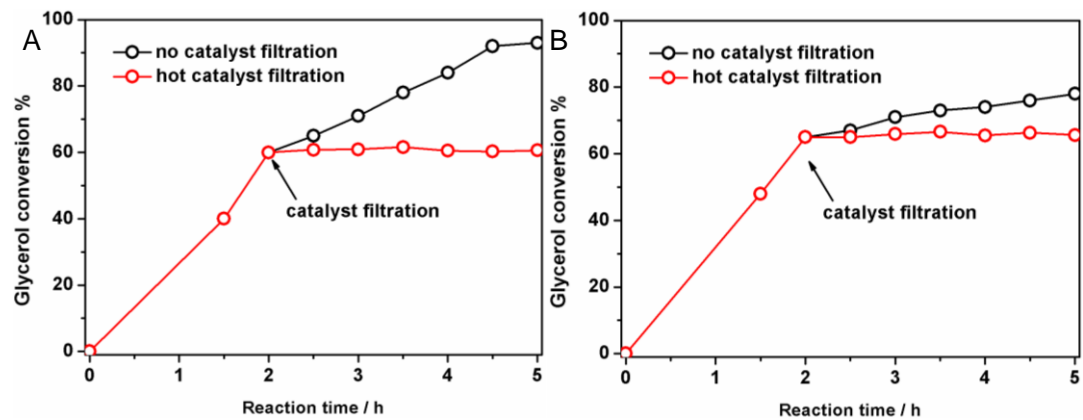
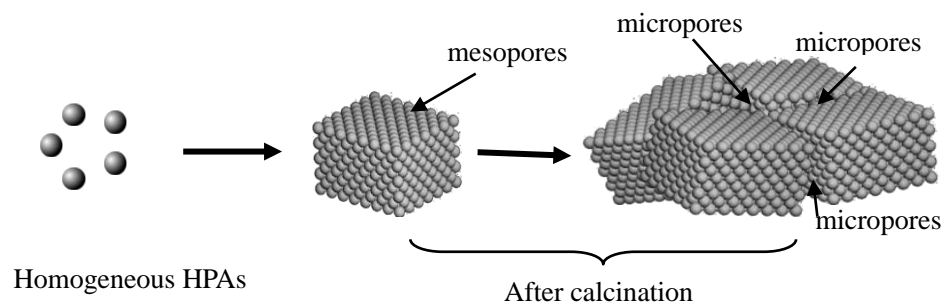
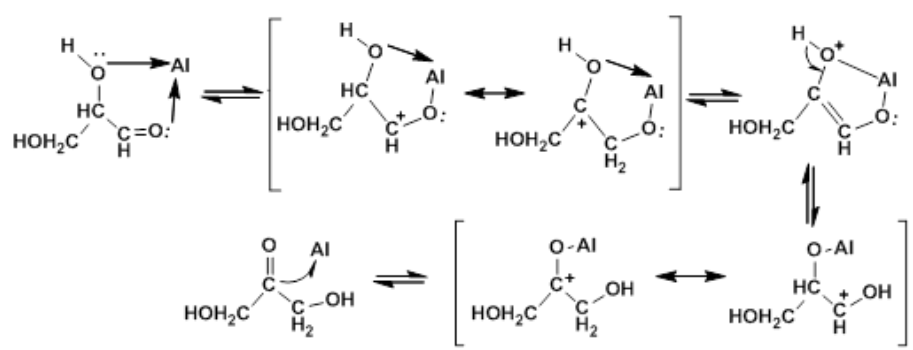


**Fig S17.** Leaching experiment of heterogeneous catalyst: AlPMo<sub>12</sub> (A) and HPMo<sub>11</sub>Al (B).

Reaction conditions: 5 mL of 1.0 M glycerol, 4.0 mM catalyst, 60 °C, 1 MPa O<sub>2</sub>, 5 h, 800 rpm.



**Scheme S1.** The formation mode of mesopores and micropores.



**Scheme S2.** The mechanism of  $\text{Al}^{3+}$  catalytic isomerization of GCA to DHA

**Table S1** Summarize of glycerol oxidation

Cat.	Oxident	Conditions	CON. %	Sel. %	Ref.
Pt-Bi/charcoal	air	50 °C, 4 h	80	DHA (80)	6
Au/charcoal	O <sub>2</sub>	60 °C, 3 h	56	GlyA (100)	7
Pt/Chloride	air	30 °C, 8 h	80	GlyA (56.9)	8
Bi-Pt/C	air	60 °C, 5 h	75	DHA (50)	9
1% Pt/C	O <sub>2</sub>	50 °C, 4 h	81.6	GlyA (50)	10
Au-Pt/C	O <sub>2</sub>	60°C, 1.5h	50	DHA (72)	11
5%Pt/C	Air	60 °C, 21 h	60	GlyA (48)	12
1% Au/C	O <sub>2</sub>	30 °C, 20h	100	GlyA (92)	13
5%Pt-5%Bi/C	O <sub>2</sub>	60 °C, 6 h	91.5	DHA (49)	14
Pd-on-Au/C	O <sub>2</sub>	60 °C, 3h	98	GlyA (43)	15
AuPd/C	O <sub>2</sub>	60 °C, 5h	50	GlyA (84)	16
CuAlMg/C	O <sub>2</sub>	60 °C, 3h	97.3	GlyA (70)	17
Pt-Cu/C	O <sub>2</sub>	60 °C, 6h	86.2	GlyA (70.8)	18
Pt/C	O <sub>2</sub>	60 °C, 6h	50	GlyA (47.4)	19
Pt/C	O <sub>2</sub>	6h	20.4	GlyA (45)	20
Pt-Bi/C	O <sub>2</sub>	70 °C, 8h	80	DHA (48)	21
Pd/graphite	O <sub>2</sub>	50 °C, 1 h	90	GlyA (62)	22
Pt/MCN	O <sub>2</sub>	60 °C, 4h	63.1	GlyA (58.5)	23
Pt/CNTs	O <sub>2</sub>	60 °C, 9 h	63	GlyA (37.6)	24
PVA/Au	H <sub>2</sub> O <sub>2</sub>	50 °C	60.7	GCA (54.5)	25
Pt/ZrO <sub>2</sub>	He	180 °C, 24h	95	LA (84)	26
AuPt/MCM-41	O <sub>2</sub>	80°C, 0.25h	30	GCA (46)	27
Pt/AC <sub>PO</sub>	O <sub>2</sub>	60 °C, 6h	55	GlyA (35.3)	28
Pt/TiO <sub>2</sub>	O <sub>2</sub>	90 °C, 2h	10	GCA (67.2)	29
Pt-PVP+TiO <sub>2</sub>	O <sub>2</sub>	150 °C, 18h	100	LA (63)	30
Ru-Zn-Cu <sup>I</sup> /HAP	O <sub>2</sub>	140 °C, 12h	100	LA (82.7)	31
Pt/Sn-MFI	O <sub>2</sub>	100 °C, 24h	89.8	LA (80.5)	32
Pt NPs/HT	O <sub>2</sub>	60 °C, 6h	80	GlyA (40)	33
10%Ni/ $\gamma$ -Al <sub>2</sub> O <sub>3</sub>	5%H <sub>2</sub>	300 °C, 6 h	50	CH <sub>4</sub> (100)	34
Ti-Si co-gel	H <sub>2</sub> O <sub>2</sub>	80 °C, 24 h	22	GCA (37)	35
CuO/ZrO <sub>2</sub>	N <sub>2</sub>	180 °C, 8h	100	LA (94.6)	36
Au/MgO-Al <sub>2</sub> O <sub>3</sub>	O <sub>2</sub>	80°C, 0.5h	16.4	DHA (74)	37
LDH[Cr (SO <sub>3</sub> salen) ]	H <sub>2</sub> O <sub>2</sub>	60°C, 4h	71.3	DHA (43.5)	38
Urea-Gluconobacter		30 °C, 6h	84.8	DHA (96.4)	39
H <sub>4</sub> PV <sub>1</sub> Mo <sub>11</sub> O <sub>40</sub>	O <sub>2</sub>	150 °C, 3h	90.6	FA (41.2)	40
[LMn (u-O) <sub>3</sub> MnL] <sub>2</sub> [SiW <sub>12</sub> O <sub>40</sub> ]	H <sub>2</sub> O <sub>2</sub>	22°C, 24h	40	DHA (15.3)	41

**Table S2** Immobilization of POMs and their heterogeneous catalytic studies in different organic transformations

Cat.	Reactions	Ref.
$\text{Cs}_{2.2}\text{H}_{0.8}\text{PW}_{12}\text{O}_{40}$	decomposition of ester, dehydration of alcohol, and alkylation of aromatics	42
$\text{Cs}_3\text{PW}_{12}\text{O}_{40}$	conversions of cellobiose and cellulose into sorbitol in water	43
$\text{Ag}_3\text{PW}_{12}\text{O}_{40}$	intermolecular hydroamination of olefins	44
$\text{K}_{2.2}\text{H}_{0.8}\text{PW}_{12}\text{O}_{40}$	esterification of 2-keto-L-gulonic acid	45
$(\text{NH}_4)_3\text{PW}_{12}\text{O}_{40}$	intermolecular hydroamination of olefins	44
$\text{Sn}_x[\text{H}_{3-2x}\text{PW}_{12}\text{O}_{40}]$	benzylation of arenes with benzyl alcohol	46
$\text{Zn}_{1.2}\text{H}_{0.6}\text{PW}_{12}\text{O}_{40}$	esterification of palmitic acid and transesterification of waste cooking oil	47
$\text{BiPW}_{12}\text{O}_{40}$	esterification of oleic acid with n-butanol	48
$\text{H}_3\text{PW}_{12}\text{O}_{40}/\text{SBA}-15$	acid-base tandem reaction	49
$\text{H}_4\text{SiMo}_{12}\text{O}_{40}/\text{Mesoporous silica hollow sphere}$	Friedel-Crafts alkylation	50
$\text{Na}_7\text{H}_2\text{LaW}_{10}\text{O}_{36}/\text{IL-modified SiO}_2$	oxidative desulfurization	51
$\text{H}_3\text{PW}_{12}\text{O}_{40}/\text{MIL-101}(\text{Cr})$	carbohydrate dehydration to HMF	52
$[\text{CuPW}_{11}\text{O}_{39}]^{5-}/\text{HKUST-1}$	detoxification of various sulfur compounds	53
$\text{PMo}_{10}\text{V}_2\text{O}_{40}^{5-}/\text{PIL poly(VMCA)}$	esterification reactions	54
$\text{H}_3\text{PMo}_{12}\text{O}_{40}$ (PMA)/ Mesoporous $\text{Cr}_2\text{O}_3$	oxidation of 1-phenylethanol with $\text{H}_2\text{O}_2$	55
$\text{K}_{12.5}\text{Na}_{1.5}[\text{NaP}_5\text{W}_{30}\text{O}_{110}]/\text{RGO}$	electrolytic water oxidation	56
d/POMs/NHCSS	electrochemical induction with paracetamol	57
$\text{SiPMo}_{12}/\text{MWCNTs}$	supercapacitor	58
$\text{PMo}_{12}@\text{g-C}_3\text{N}_4$ , $\text{PW}_{12}@\text{g-C}_3\text{N}_4$	photocatalytic degradation of methylene blue and phenol	59
AC@PMo <sub>12</sub>	supercapacitor	60
FAD-GDH/P <sub>2</sub> Mo <sub>18</sub> /PMA/MWCNTs	glucose biosensor	61
POMOFs/RGO	lithium ion battery	62

**Table S3** The Lewis acidity and elementary analysis of LPMo<sub>12</sub>

Catalysts	Lewis acidity, mmol/g	Elementary results (calculated values in parenthesis)/wt%		
		<b>P</b>	<b>Mo</b>	<b>L</b>
HPMo <sub>12</sub>	0	1.62(1.69)	63.23(63.08)	-
AlPMo <sub>12</sub>	0.60	1.57(1.62)	60.44(60.04)	4.78(4.97)
FePMo <sub>12</sub>	0.48	1.59(1.65)	62.36(61.30)	2.95(2.97)
CrPMo <sub>12</sub>	0.42	1.59(1.65)	61.67(61.43)	2.74(2.77)
TiPMo <sub>12</sub>	0.40	1.62(1.67)	62.61(61.96)	2.04(1.93)
ZnPMo <sub>12</sub>	0.25	1.58(1.61)	60.75(59.95)	5.23(5.11)
ZrPMo <sub>12</sub>	0.19	1.61(1.64)	61.03(60.89)	3.56(3.62)

**Table S4** The elementary analysis of HPMo<sub>11</sub>L

Catalyst	Lewis acidity, mmol/g	Elementary results (calculated values in parenthesis)/wt%		
		P	Mo	M
HPMo <sub>12</sub>	0.03	1.52(1.60)	64.03(63.08)	-
HPMo <sub>11</sub> Al	0.52	1.74(1.78)	61.10(60.61)	1.43(1.55)
HPMo <sub>11</sub> Fe	0.48	1.69(1.75)	60.00(59.62)	3.04(3.15)
HPMo <sub>11</sub> Ti	0.39	1.71(1.74)	60.01(59.32)	2.65(2.69)
HPMo <sub>11</sub> Cr	0.28	1.69(1.75)	60.04(59.75)	2.90(2.94)
HPMo <sub>11</sub> Zn	0.15	1.70(1.74)	59.02(59.26)	3.62(3.67)

It showed that the molar ratios of P: Mo is 1:11, respectively. This indicated that the keggin structure for HPMo<sub>11</sub>L did not destroy during the introduction of Lewis metals. For HPMo<sub>11</sub>L, the molar ratio of L: Mo as 1: 11 confirmed the formation of mono-substituted molybdophosphoric acid.

**Table S5.** Oxidation of glycerol in the presence of LPMo<sub>12</sub> catalysts

Entry	Catalysts	SSA, m <sup>2</sup> /g	CON, %	yields, %					
				DHA	GCA	GlyA	PRA	LA	AcA
1	AlPMo <sub>12</sub>	12.0	93.7	2.1	1.0	3.1	1.2	84.8	3.1
2	FePMo <sub>12</sub>	11.5	90.0	3.2	3.2	2.0	1.3	80.2	1.2
3	CrPMo <sub>12</sub>	11.0	88.2	4.0	5.3	2.2	1.4	73.1	1.1
4	TiPMo <sub>12</sub>	7.5	77.0	6.3	5.1	5.1	2.0	56.0	0
5	ZrPMo <sub>12</sub>	7.2	48.4	8.1	7.0	5.1	3.1	19.2	0
6	ZnPMo <sub>12</sub>	6.3	30.1	9.0	8.2	0	3.2	10.3	0

Reaction conditions: 5 mL of 1.0 M glycerol, 4.0 mM catalyst, 60 °C, 1 MPa O<sub>2</sub>, 5 h, 800 rpm.

**Table S6.** Oxidation of glycerol in the presence of HPMo<sub>11</sub>L catalysts

Entry	Catalyst	SSA	CON	Yields, %					
		m <sup>2</sup> /g	%	DHA	GCA	GlyA	PRA	LA	AcA
1	HPMo <sub>11</sub> Al	20.1	78.1	11.2	26.1	4.2	2.1	55.0	2.1
2	HPMo <sub>11</sub> Fe	19.6	68.2	14.3	32.3	3.1	4.2	46.2	1.0
3	HPMo <sub>11</sub> Ti	19.2	50.1	20.1	39.0	4.3	5.0	32.3	0
4	HPMo <sub>11</sub> Cr	19.4	31.0	25.1	50.2	0	9.3	16.2	0
5	HPMo <sub>11</sub> Zn	18.9	16.2	26.0	59.1	0	6.0	9.1	0

Reaction conditions: 1 M glycerol, 4 mM catalyst, 60 °C, 5 h, 1 MPa O<sub>2</sub>, 800 rpm.

**Table S7** The acidity mesurement of LPMo<sub>12</sub>

Catalysts	Lewis acidity (mmol/g)	Brønsted acidity (mmol/g)	B / L
AlPMo <sub>12</sub>	0.60	0.05	0.1
Al <sub>0.67</sub> PMo <sub>12</sub>	0.42	0.33	0.8
Al <sub>0.33</sub> PMo <sub>12</sub>	0.25	0.65	2.6
FePMo <sub>12</sub>	0.48	0.04	0.1
Fe <sub>0.67</sub> PMo <sub>12</sub>	0.34	0.31	0.9
Fe <sub>0.33</sub> PMo <sub>12</sub>	0.18	0.63	3.5

**Reference**

- [1] C. A. Emeis, J Catal. 1993, 141, 347-354.
- [2] V. L. Budarin, J. H. Clark, R. Luque, D. J. Macquarrie, A. Koutinas and C. Webb, Green Chem. 2007, 9, 992-995.
- [3] N. Dimitratos, J. C. Vedrine, J Mole Catal A: Chem. 2006, 255, 184-192.
- [4] H. Zhang, T. Wang, X. Ma, W. Zhu, Catalysts 2016, 6, 187-199.
- [5] C. R. Deltcheff, R. Thouvenot, R. Frank, Spectrochim. Acta A. 1976, 32, 587-597.
- [6] H. Kimura, K. Tsuto, T. Wakisaka, Y. Kazumi, Y. Inaya, Appl Catal A: Gen. 1993, 96, 217-228.
- [7] S. Carrettin, P. McMorn, P. Johnston, K. Griffin, G. J. Hutchings. Chem Commun. 2002, 7, 696-697.
- [8] M. S. Gross, B. S. Sanchez, C. A. Querini. Appl Catal A: Gen. 2015, 501, 1-9.
- [9] R. Garcia, M. Besson, P. Gallezot, Appl Catal A: Gen. 1995, 127, 165-176.
- [10] N. Dimitratos, C. Messi, F. Porta, L. Prati, A. Villa, J Mol Catal A: Chem. 2006, 256, 21-28.
- [11] S. Demirel, K. Lehnert, M. Lucas, P. Claus, Appl Catal B: Environ. 2007, 70, 637-643.
- [12] S. Carrettin, P. McMorn, P. Johnston, K. Griffin, C. J. Kiely, G. J. Hutchings, Phys Chem Chem Phys. 2003, 5, 1329-1336.
- [13] F. Porta, L. Prati, J Catal. 2004, 224, 397-403.
- [14] D. Liang, S. Cui, J. Gao, J. Wang, P. Chen, Z. Hou, Chin J Catal. 2011, 32, 1831-1837.
- [15] Z. Zhao, J. Arentz, L. A. Pretzer, P. Limpornpipat, J. M. Clomburg, R. Gonzalez, N. M. Schweitzer, T. Wu, J. T. Miller, M. S. Wong, Chem Sci. 2014, 5, 3715-3728.
- [16] W. C. Ketchie, M. Murayama, R. J. Davis, J Catal. 2007, 250, 264-273.
- [17] C. H. Zhou, J. N. Beltramini, C. X. Lin, Z. P. Xu, G. Q. Lu, A. Tanksale, Catal Sci Technol. 2011, 1, 111-122.
- [18] D. Liang, J. Gao, J. Wang, P. Chen, Y. Wei, Z. Hou, Catal Commun. 2011, 12, 1059-1062.
- [19] D. Liang, J. Gao, J. Wang, P. Chen, Z. Hou, X. Zheng, Catal Commun. 2009, 10, 1586-1590.
- [20] Z. Zhang, L. Xin, W. Li, Appl Catal B: Environ. 2012, 119-120, 40-48.
- [21] W. Hu, D. Knight, B. Lowry, A. Varma, Ind Eng Chem Res. 2010, 49, 10876-10882.
- [22] N. Dimitratos, F. Porta, L. Prati, Appl Catal A: Gen. 2005, 291, 210-214.

- [23] F. F. Wang, S. Shao, C. L. Liu, Chml Eng J. 2015, 264, 336-343.
- [24] J. Lei, X. Duan, G. Qian, X. Zhou, D. Chen, Ind Eng Chem Res. 2014, 53, 16309-16315.
- [25] C. A. Nunes, M. C. Guerreiro, J Mol Catal A: Chem. 2013, 370, 145-151.
- [26] J. Ftouni, N. Villandier, F. Auneau, M. Besson, L. Djakovitch, C. Pinel, Catal Today. 2015, 257, 267-273.
- [27] A. Villa, S. Campisi, K. M. H. Mohammed, N. Dimitratos, F. Vindigni, M. Manzoli, W. Jones, M. Bowker, G. J. Hutchings, L. Prati, Catal Sci Technol. 2015, 5, 1126-1132.
- [28] J. Lei, H. Dong, X. Duan, W. Chen, G. Qian, D. Chen, X. Zhou, Ind. Eng. Chem. Res. 2016, 55, 420-427.
- [29] Y. Shen, Y. Li, H. Liu, J Energy Chem. 2015, 24, 669-673.
- [30] T. Komanoya, A. Suzuki, K. Nakajima, M. Kitano, K. Kamata, M. Hara, ChemCatChem. 2016, 8, 1094-1099.
- [31] Z. Jiang, Z. Zhang, T. Wu, P. Zhang, J. Song, C. Xie, B. Han, Chem Asian J. 2017, 12, 1598-1604.
- [32] H. J. Cho, C. C. Chang, W. Fan, Green Chem. 2014, 16, 3428-3433.
- [33] D. Tongsakul, S. Nishimura, C. Thammacharoen, S. Ekgasit, K. Ebitani, Ind Eng Chem Res. 2012, 51, 16182-16187.
- [34] B. C. Miranda, R. J. Chimentão, J. B. O. Santos, F. Gispert-Guirado, J. Llorca, F. Medina, F. L. Bonillo, J. E. Sueiras, Appl Catal A: Gen. 2014, 147, 464-480.
- [35] P. McMorn, G. Roberts, G. J. Hutchings, Catal Lett. 1999, 63, 193-197.
- [36] G. Y. Yang, Y. H. Ke, H. F. Ren, C. L. Liu, R. Z. Yang, W. S. Dong, Chem Eng J. 2016, 283, 759-767.
- [37] Z. Yuan, Z. Gao, B. Q. Xu, Chin J Catal. 2015, 36, 1543-1551.
- [38] X. Wang, G. Wu, F. Wang, K. Ding, F. Zhang, X. Liu, Y. Xue, Catal Commun. 2012, 28, 73-76.
- [39] Z. C. Hu, S. Y. Tian, L. J. Ruan, Bioresource Technol. 2017, 233, 144-149.
- [40] J. Zhang, M. Sun, Y. Han RSC Adv. 2014, 4: 35463-35466.
- [41] G. B. Shul'pin, Y. N. Kozlov, L.S. Shul'pina, T. V. Strelkova, D. Mandelli, Catal Lett. 2010, 138, 193-204.
- [42] O. Toshio, N. Toru, M. Makoto. Chem Lett. 1995, 24, 155-156.
- [43] W. Shi, J. Zhao, X. Yuan, S. Wang, X. Wang, M. Huo, Chem Eng Technol. 2012, 35, 347-352.
- [44] L. Yang, L. W. Xu, C. G. Xia. Tetrahedron Lett. 2008, 49, 2882-2885.
- [45] T. H. T. Vu, H. T. Au, T. M. T. Nguyen, M. T. Pham, T. T. Bach, H. N. Nong, Catal Sci Technol. 2013, 3, 699-705.
- [46] C. R. Kumar, K. T. V. Rao, P. S. S. Prasad, N. Lingaiah, J Mol Catal A: Chem. 2011, 337, 17-24.
- [47] J. Li, X. Wang, W. Zhu, F. Cao, ChemSusChem. 2009, 2, 177-183.
- [48] J. Wang, G. Luo, C. Liu, J. Lai, Energy Sources Part A. 2014, 36, 479-488.
- [49] K. Inumaru, T. Ishihara, Y. Kamiya, T. Okuhara, S. Yamanaka, Angew Chem Int Ed. 2007, 46,

7625-7628.

- [50] J. Dou, H. C. Zeng, *J Am Chem Soc.* 2012, 134, 16235-16246.
- [51] Y. Chen, Y. Song, *ChemPlusChem.* 2014, 79, 304-309.
- [52] Y. Zhang, V. Degirmenci, C. Li, E. J. M. Hensen, *ChemSusChem.* 2011, 4, 59-64.
- [53] J. Song, Z. Luo, D. K. Britt, H. Furukawa, O. M. Yaghi, K. I. Hardcastle, C. L. Hill, *J Am Chem Soc.* 2011, 133, 16839-16846.
- [54] Y. Leng, P. Jiang, J. Wang, *Catal Commun.* 2012, 25, 41-44.
- [55] F. Su, L. Ma, Y. Guo, W. Li, *Catal Sci Technol.* 2012, 2, 2367-2374.
- [56] M. Jiang, D. Zhu, J. Cai, H. Zhang, X. Zhao, *J Phys Chem C.* 2014, 118, 14371-14378.
- [57] L. Wang, T. Meng, J. Sun, S. Wu, M. Zhang, H. Wang, Y. Zhang, *Anal Chim Acta.* 2019, 1047, 28-35.
- [58] T. Akter, K. Hu, K. Lian, *Electrochim Acta.* 2011, 56, 4966-4971.
- [59] J. He, H. Sun, S. Indrawirawan, X. Duan, M. O. Tade, S. Wang, *J Colloid Interface Sci.* 2015, 456, 15-21.
- [60] C. Hu, E. Zhao, N. Nitta, A. Magasinski, G. Berdichevsky, G. Yushin, *J Power Sources.* 2016, 326, 56-74.
- [61] F. Boussema, A. J. Gross, F. Hmida, B. Ayed, H. Majdoub, S. Cosnier, A. Maaref, M. Holzinger, *Biosens Bioelectron.* 2018, 109, 20-26.
- [62] T. Wei, M. Zhang, P. Wu, Y. J. Tang, S. L. Li, F. C. Shen, X. L. Wang, X. P. Zhou, Y. Q. Lan, *Nano Energy.* 2017, 34, 205-214.